Facilitating suitable design decisions for an industrial energy system considering rule-based energy management systems: A brewery case study

Johannes B. Lipka [,a,b], Lukas Höttecke [a], Paul Stursberg [a], Michael Metzger [a] and Stefan Niessen [a,b]*

[a] *Foundational Technologies, Siemens AG, Otto-Hahn-Ring 6, Munich 81739, Bavaria, Germany*
[b] *Technology and Economics of Multimodal Energy Systems, TU Darmstadt, Landgraf-Georg-Str. 4, Darmstadt, 64283, Hessen, Germany*
[*] *johannes-bernd.lipka@siemens.com* ***(CA)***

Abstract

Decarbonization of industrial sites requires substantial investments in on-site infrastructure. This paper presents a control-informed design optimization (CID_0) framework for industrial energy systems, explicitly accounting for rule-based energy management strategies commonly applied in practice. Using a brewery case study, the approach is compared to conventional design optimization (D_0), which assumes perfect operational foresight and flexibility utilization. The results show that D_0 installs approximately 4.5 MWp of PV and only limited additional storage, but when this design is re-simulated under reactive rule-based control, annual TOTEX increases by 29.6% and PV curtailment rises from 1.1% to 88.0%. In contrast, CID_0 yields a markedly different design with about 860 kWp of PV, 813 kWh of additional BESS and 815 kWh of additional HWT capacity. When re-simulated under rule-based control, the resulting TOTEX increase is limited to 6.9%, while PV curtailment rises from 8.8% to 57.6%. Further analysis of storage full cycles and asset full load hours shows that the discrepancies are mainly caused by the inability of reactive rule-based control to exploit temporal flexibility in the same way as idealized co-optimization. The findings demonstrate that neglecting operational constraints can lead to misleading investment decisions and that effective renewable integration requires control-aware design and, for high renewable shares, more sophisticated energy management strategies.

Keywords:

Design optimization; Energy management systems; Control strategy.

1. Introduction

Industrial energy systems play a pivotal role in global decarbonization efforts due to their substantial contribution to overall energy consumption and greenhouse gas emissions [1]. Energy-intensive sectors, including manufacturing and food processing, depend on tightly integrated thermal and electrical processes, presenting both challenges and opportunities for efficiency improvements and renewable energy integration. The growing penetration of intermittent renewable sources, such as photovoltaic (PV) systems, further increases the need for enhanced flexibility and coordinated system operation [2]. Optimization-based methods are widely applied to support the design and operation of such systems, typically employing mathematical programming to identify cost-optimal configurations and strategies [3].

However, these approaches frequently rely on assumptions of perfect foresight and full operational flexibility, which are seldom achievable in real industrial contexts. In practice, energy systems are often managed by rule-based energy management systems (EMS) [4], where predefined priorities govern asset dispatch without predictive capabilities. This discrepancy between theoretical models and practical operation can result in misleading design outcomes, with studies showing that perfect foresight assumptions may overestimate economic viability resulting from lower renewable utilization rates. Consequently, integrating a more realistic operational behavior into the design phase is essential to ensure robust and implementable solutions.

1.1. Relevant work and literature review

Recent reviews show that the design of multi-energy systems has increasingly converged on mixed-integer linear programming (MILP) and related mathematical-programming approaches because they are able to co-optimize discrete investment decisions and chronological operation across electricity, heat, cooling, and storage [3]. This is particularly relevant for industrial sites, where CHP, boilers, heat pumps, chillers, storage, and external energy procurement must be coordinated under detailed asset models including part-load ratios, and complex tariff structures [5]. Foundational industrial studies such as Atabay's open-source factory model [6], the MIND framework [7], and industrial energy-hub formulations [8] established MILP as a practical way to represent multi-commodity balances, unit commitment, and cost-optimal dispatch in industrial energy systems.

At the same time, the literature repeatedly highlights a methodological weakness in design optimization: many studies solve a single deterministic problem over the full horizon and therefore assume perfect foresight of future demands, prices, and renewable availability. Urban et al. [5] note that model suitability for engineering practice depends strongly on how the design process is represented, while Cuisinier et al. [9] show that operational modelling choices such as foresight, temporal resolution, and technology modelling detail affect techno-economic conclusions. More recently, Brisson et al. [10] demonstrate that the modelling detail assigned to the control strategy itself can alter the sizing optimum, which is directly relevant to systems that include PV, batteries, and thermal storage.

This issue is especially important for renewable integration and storage valuation. The apparent value of PV, batteries, and thermal storage in simultaneous design-and-dispatch optimization depends on anticipatory charging, discharging, and peak-shaving decisions that are often unavailable under practical plant control. Reviews focused on flexibility and robustness further show that many local and integrated energy-system models still underrepresent technical flexibility in ways that matter most when intermittent renewables become prominent. In other words, an optimizer may identify a mathematically attractive design whose value partly rests on operational freedom that the deployed EMS cannot actually realize [9–11].

The gap between optimized and realized performance is therefore also a control problem. Field-oriented EMS research shows that rule-based strategies remain common because they are transparent, robust and easier to implement within existing hardware, software, and communication constraints, whereas optimization-based EMS require better forecasts, stronger models, and more integration effort [4]. Restrepo et al. [12] explicitly compare rule-based and optimization-based EMS in a real microgrid facility and note that rule-based EMS is still typical in deployed controllers, while [4] recently demonstrated that MILP-based MPC can be implemented successfully in a real industrial food-processing plant. These studies suggest that advanced predictive control can unlock additional flexibility, but they also confirm that practical operation often remains far more constrained than the ideal dispatch assumed in design optimization.

Against this background, there is still limited literature that directly embeds realistic rule-based control logic into the design optimization of industrial multi-energy systems. Most existing studies either optimize design under idealized operational assumptions or assess control strategies after the design has already been fixed. For industrial sites such as breweries, where steam, hot water, cooling, electricity, PV, and storage are tightly coupled, the relevant question is therefore not only which design is optimal under perfect foresight, but which design remains robust once it is operated under the actual EMS. This is the gap addressed in the present work.

1.2. Contributions

This study aims to bridge the gap between energy system design and real-world operation by incorporating rule-based control strategies into the optimization framework. The main contributions are:

- Development of a MILP control-informed design framework that embeds rule-based EMS logic into the sizing problem.
- A comparative evaluation against conventional full-foresight design optimization and subsequent re-simulation under reactive rule-based control (RRBC).
- A quantitative brewery case study showing the impact of neglecting operational constraints on TOTEX, PV sizing, BESS sizing, and PV curtailment.

By aligning design optimization with practical operation, the proposed framework supports more reliable and implementable investment decisions in industrial energy systems.

2. Mathematical model

This section presents the MILP-based formulation used to represent system dynamics, perform design optimization, and incorporate rule-based operational control.

2.1. System dynamics and design optimization

The underlying MILP design optimization framework is extensively described in [13] and previously applied in [14-16]. For brevity, only the cost formulation is summarized here.

In design optimizations, total annual system costs, comprising annualized investment and operational costs across all assets $k \in \mathcal{K}$, are minimized in Eq. (1). The annuity af_k of each asset k depends on the interest rate r and its technical lifetime n_k.

$$\min \sum_{k \in \mathcal{K}} af_k \cdot \zeta_k^{\mathrm{Inv}} + \zeta_k^{\mathrm{Opr}} . \tag{1}$$

$$af_k = \frac{r^{n_k}(r-1)}{r^{n_k}-1} \tag{2}$$

This formulation optimizes system design and operation simultaneously over a full year within a single iteration. The assumption of perfect foresight enables optimal handling of time-coupled constraints, such as peak loads and storage dispatch. However, such prescient operation is rarely achievable in practice. Instead, most industrial systems rely on reactive rule-based control strategies.

2.2. Reactive rule-based control

Existing industrial energy management systems are mostly based on a reactive rule-based control strategy where the system determines which demands will be addressed first and which assets will be committed first to cover these commodities based on an operator's predefined sequence. This operational paradigm contrasts with the assumption in Section 2.1, i.e., design studies generally presuppose an optimal system-wide allocation of assets at each time step.

These strategies can vary significantly depending on static rules defined by the commissioning engineer. For example, a CHP unit may be run heat- or electricity-led. Moreover, assets (e.g., heat pumps, boilers, storage) may be operated with different priorities. In this section, this practical dispatch logic is translated into a MILP-based model that represents rule-based control strategies in the context of an optimization-based framework like the one described in Sec. 2.1.

2.2.1 Commodity priority

Industrial energy systems comprise multiple energy demands associated with individual control loops. To reflect this nested structure, each primary energy commodity $c \in \mathbb{C}^p$, e.g., steam, electricity, is assigned a priority weight w^c. These weights define which type of demand is satisfied first, with higher values meaning higher priority. For example, if steam is to be supplied before electricity, then $w^{\mathrm{steam}} > w^{\mathrm{electricity}}$. This ensures the optimizer always allocates resources to higher priority demands first. In reality, all commodities shall be supplied reliably at any time step. Nonetheless, this formulation helps us model heat- or electricity-led operation, e.g., of a CHP, by adjusting the priority weights of commodity steam and commodity electricity. These weights later enter the priority cost formulation in Eq. (4), where higher commodity weights increase the penalty associated with leaving that commodity unsupplied and thereby enforce the intended dispatch order within each rolling-horizon optimization step.

2.2.2 Asset priority

For each primary commodity c, multiple assets may be able to supply it, e.g., boiler, CHP, heat pump. Each of those assets, $k \in K_{\mathrm{Out}}^c$, is then assigned a secondary weight w_k^c. These define the order of asset dispatch within the same commodity, with a lower value indicating a higher priority, i.e., asset is used first. For example, in the case of steam supply, $w_{\mathrm{CHP}}^{\mathrm{steam}} < w_{\mathrm{boiler}}^{\mathrm{steam}} < w_{\mathrm{el.\ boiler}}^{\mathrm{steam}}$ enforces a sequence of $\mathrm{CHP} \rightarrow \mathrm{gas\ boiler} \rightarrow \mathrm{electric\ boiler}$.

Energy storage systems require special treatment because they can both consume (charge) and supply (discharge) energy. Discharging weights w_k^c behave like normal asset weights with positive values. Charging weights $w_{k,\,\mathrm{ch}}^c$ are negative, which ensures charging happens only under preferred conditions. This induces a

controlled operating behaviour where storage is charged only when surplus energy is available and discharge follows a defined priority order. For example, the hierarchy $w^{\text{hot water}}_{\text{heat pump}} < |w^{\text{hot water}}_{\text{storage, ch}}| < w^{\text{hot water}}_{\text{gas boiler}} < w^{\text{hot water}}_{\text{storage}}$ results in the heat pump being prioritized for covering the hot water demand. If available capacity remains, then storage is charged. If the heat pump cannot supply all of the hot water demand, then the gas boiler is dispatched and last, the storage is discharged as a last resort. The sequence presented here is intended solely as an illustrative example to facilitate understanding of storage priorities and does not necessarily reflect a practically meaningful scenario.

2.2.3 Priority cost formulation

In order to model a reactive rule-based operation of the system, the system is simulated using a rolling horizon approach. Let $\mathbb{T}$ denote the set of optimization time steps with cardinality $|\mathbb{T}|$. For example, a yearly optimization with hourly resolution results in $|\mathbb{T}| = 8760$. At each time step $t \epsilon \mathbb{T}$, a priority-based objective function, see Eq. (3), is minimized, after which the horizon is shifted, and the optimization is repeated for the next timestep $t^{\text{new}} = t + 1$.

$$\min \sum_{c \in \mathbb{C}^p} \zeta_c^{\text{Priority}}(t) \tag{3}$$

The priority cost at time step t, $\zeta_c^{\text{Priority}}(t)$, is defined as follows:

$$\zeta_c^{\text{Priority}}(t) = w^c L^c(t) \sum_{k \in K^c_{\text{Out}}} w^c_k P^{\text{Out}}_{k,c}(t), \tag{4}$$

with

$$L^c(t) = \max\left(1, \sum_{k \in K^c_L} l_{k,c}(t)\right)^{-1}. \tag{5}$$

K^c_L is the set of all the loads k that consume commodity c, and $l_{k,c}(t)$ the commodity demand of load k at time step t. The priority contribution of each commodity is thus calculated using the sum of outputs from supplying assets $k \in K^c_{\text{Out}}$, multiplied by the commodity priority weight w^c and scaled by the normalization factor $L^c(t)$. This normalization factor term ensures numerical stability and independence from system size, e.g., MW-scale and kW-scale systems, allowing weights to be chosen purely on relative priorities and not absolute values.

2.3. Control-informed design optimization

Conventional design optimization assumes idealized asset operation over the entire planning horizon. To reduce this discrepancy, a control-informed design optimization framework is proposed in Figure 1, incorporating rule-based operational constraints from simulation of rule-based control into the design stage.

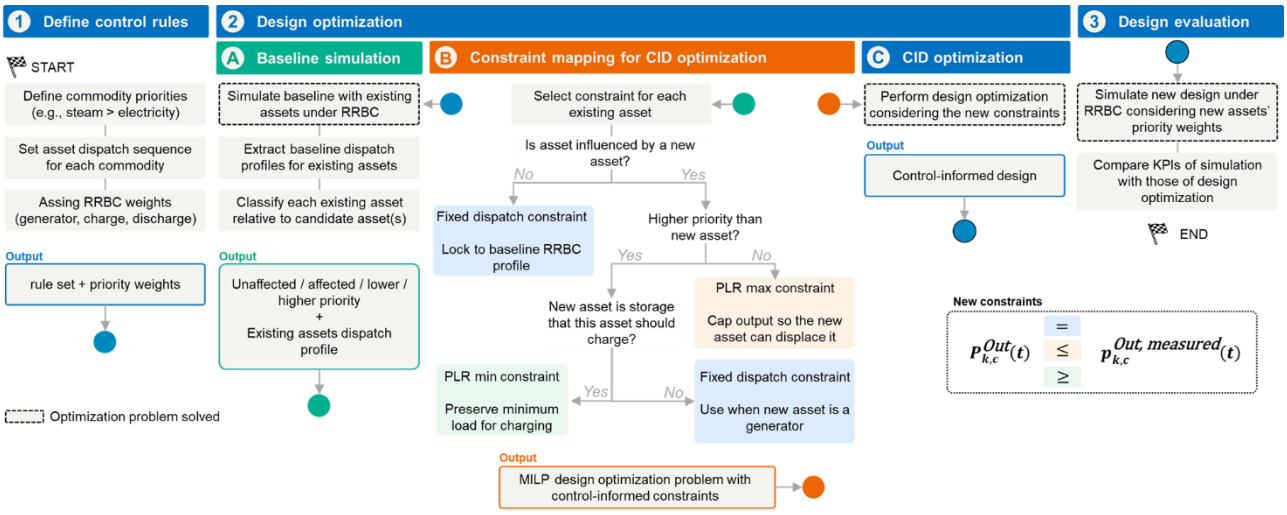

Figure 1. *Flow diagram of the control-informed design optimization framework under rule-based control.*

A brownfield system with existing assets $\mathcal{K}^{\text{existing}}$ and candidate assets $\mathcal{K}^{\text{new}}$ is considered. First, each commodity and their assets are assigned a priority weight according to Section 2.2. Then, based on the aforementioned rule-set and weights, the baseline system is simulated using RRBC to obtain reference dispatch profiles $p_{k,c}^{\text{Out, measured}}(t)$ for all time steps. Subsequently, based on the assets' priority weights w_k^c, assets are classified relative to newly installed assets.

2.3.1 Unaffected assets

Assets whose operation is unaffected by the installation of the new assets, e.g. may supply a different commodity which is uncoupled by the commodities the new assets use, have a fixed operation based on the profiles obtained from the baseline simulation, ensuring consistency with existing logic:

$$P_{k,c}^{\text{Out}}(t) = p_{k,c}^{\text{Out, measured}}(t) \tag{6}$$

2.3.2 Affected assets with higher priority

For affected assets that have higher priority compared to the new assets we define two cases: new asset is a storage or a generator. If the new asset is a storage which should be charged by the current asset, then the current asset's minimum operation is constrained by its baseline profile.

$$P_{k,c}^{\text{Out}}(t) \geq p_{k,c}^{\text{Out, measured}}(t), \tag{7}$$

If the new asset is either a storage that should not be charged by the current asset, or a generator, then its operation is not affected by the new asset and thus Eq. (6) holds again.

2.3.3 Affected assets with lower priority

Assets dispatched after new assets, i.e., with lower priority, are directly influenced by their operation. Their output is consequently reduced depending on the preceding assets. This is modelled by constraining their maximum output at each time step:

$$P_{k,c}^{\text{Out}}(t) \leq p_{k,c}^{\text{Out, measured}}(t). \tag{8}$$

2.3.4 Handling conflicting constraints

Depending on the system's structure and the interaction between several candidate assets, more than one surrogate constraint may be generated for the same existing asset. To avoid contradictions, these constraints are combined according to the following precedence rules.

Equality from Eq. (6) combined with inequality from Eq. (7) or Eq. (8): in this case, the inequality is retained and the equality is discarded. The rationale is that, although one candidate asset may leave the operation of the existing asset unchanged, another candidate asset may still impose an inherent directional effect on its dispatch. For example, an added PV unit may not affect an existing heat pump, whereas new thermal storage charged by that heat pump may require its output to be at least as high as in the original system. The inequality therefore captures the more informative and operationally relevant relationship.

Lower bound from Eq. (7) combined with upper bound from Eq. (8): when both bounds arise simultaneously, the combined surrogate constraint is omitted. Although each bound is individually meaningful, their joint imposition may artificially restrict the asset to its original dispatch pattern, which is not generally justified. For instance, additional PV generation may reduce electricity purchases from the spot market, while a new heat pump may increase them. Enforcing both bounds together would effectively impose an equality that need not hold in the redesigned system. In such cases, the constraint is therefore removed, and the optimizer is allowed to determine the appropriate dispatch.

3. Case study

The brewing industry, characterized by complex interactions between electrical and thermal energy flows, provides a relevant case for applying the aforementioned framework. The studied brewery has an annual production of about 750,000 hectolitres with energy demand derived from real operational data with a 15-

minute temporal resolution. Although based on a specific facility, the framework is designed to be scalable and applicable to other industrial sites with different configurations.

The brewery's energy consumption is summarized in Table 1, with a sample week illustrated in Figure 2(a). Due to confidentiality agreements, certain load profiles have been consolidated into main commodity categories, and only representative one-week segments are presented for illustration.

Table 1. *Commodity annual consumption breakdown in the brewery*

Commodity consumption in GWh / year End Consumer	Cooling	Electricity	Steam	Hot water
Cooling	14.3	2.7		
Brewhouse			4.5	2.8
Packaging			8.1	
Rest		5.6		4.5
Sum	**14.3**	**8.3**	**12.6**	**7.3**

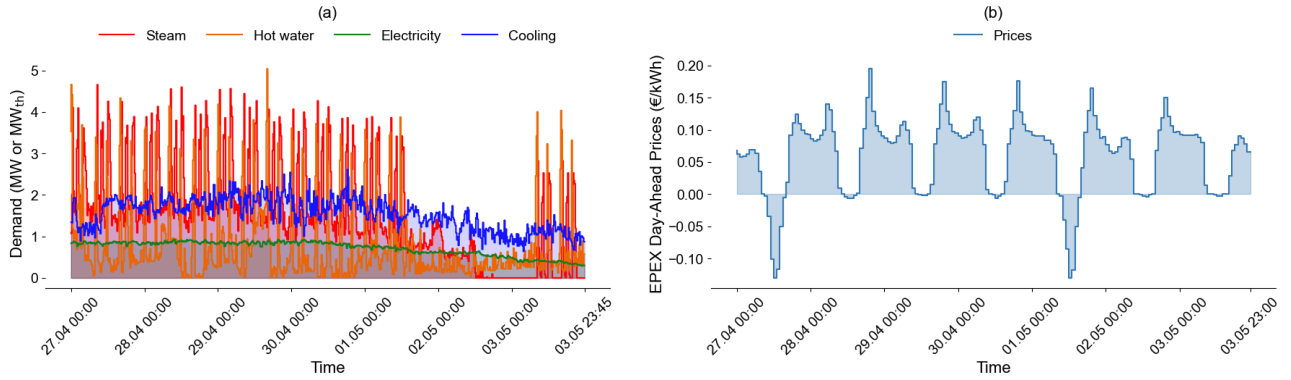

Figure. 2. *(a) Representative weekly energy demand time series for the considered brewery. (b) Exemplary weekly spot market electricity prices time series in Germany, 2025.*

3.1. Brewery's energy system topology

The brewery's energy system integrates grid supply, on-site generation, and energy storage. The system topology is illustrated in Figure 3, with key parameters summarized in Table A.1 (Appendix).

3.1.1 Electricity supply

The base load is secured through a fixed-price 300 kW futures contract at 7.96 ct/kWh. Residual demand is procured on the day-ahead market (see Figure 2.b). A heat-led CHP unit also generates electricity, which can be directly consumed, stored, or exported at 90% of the day-ahead spot price. Additional costs arise at the point of common coupling (PCC), including capacity charges of 12 €/kW/month and grid fees of 2.24 ct/kWh.

3.1.2 Cooling and heat supply

Cooling is provided by a 6.5 MW_{th} compression chiller with an annual COP of 5.2. The system offers substantial waste heat recovery potential, with approximately 67% recovered at 45°C. Thermal energy (steam and hot water) is generated by a 3 MW_{th} gas boiler (95% efficiency), a 4 MW_{th} electric boiler (98% efficiency), and a 1.2 MW_{th} CHP unit with 44.6% thermal and 42.2% electrical efficiency. Recovered heat from the chiller is upgraded to 90°C via an 800 kW_{th} heat pump (COP 3.68). A heat exchanger can further reduce temperature from 130°C to 90°C.

3.1.3 Energy storage systems

The system includes a 620 kW / 620 kWh battery energy storage system (BESS), with charging and discharging efficiencies of 95% and 89.5%, respectively. In addition, a 3 MW / MWh hot water tank (HWT) and

a 2 MW / MWh ambient water tank (AWT) enhance flexibility, enable load shifting, and improve overall efficiency. Both thermal storage systems exhibit self-discharge losses of 1% per hour.

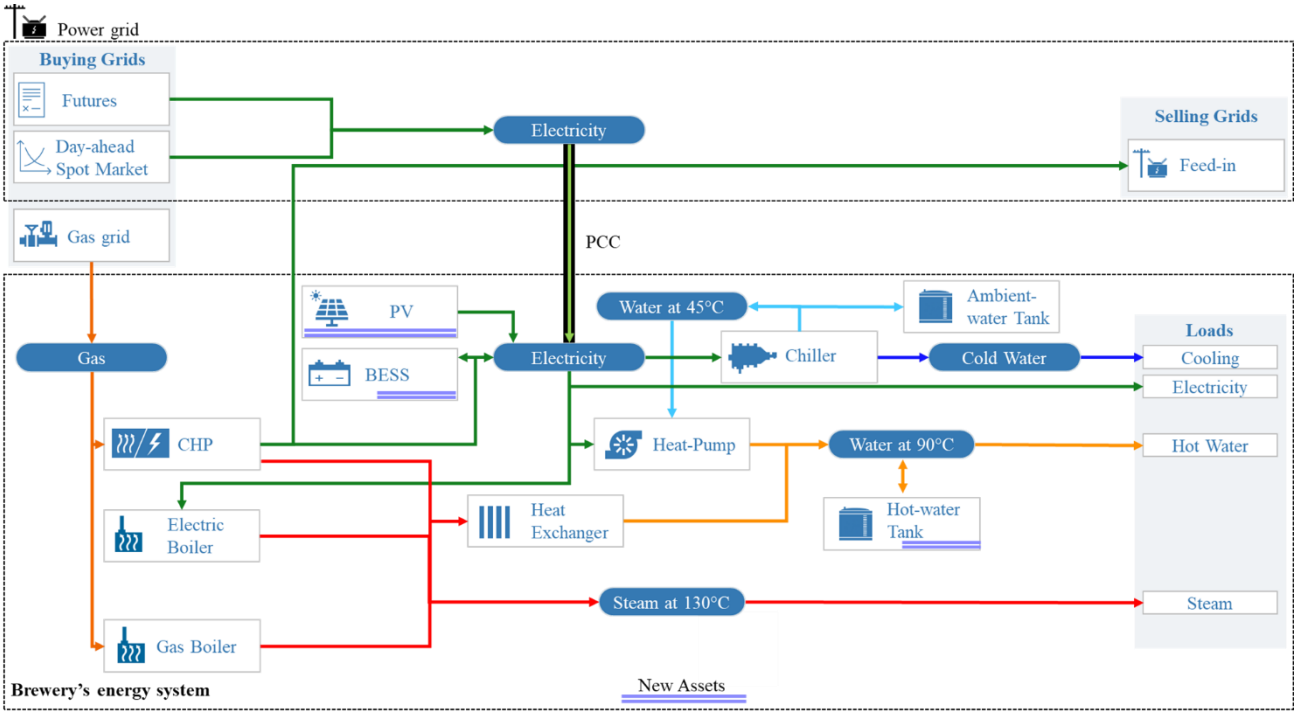

Figure. 3. *Brewery's industrial multi-modal energy system topology considered in this case study.*

3.2. Brewery's rule-based energy management system

Reactive rule-based control reflects the brewery's current operating strategy and is implemented using predefined priority rules. The system manages four main energy demands: steam, hot water, electricity, and cooling, following a hierarchy driven primarily by thermal needs. Steam demand is satisfied first using CHP, followed by the gas boiler and then the electric boiler. For hot water, the heat pump (if low-temperature heat is available) is prioritized, with excess capacity used to charge the hot water tank. If additional supply is required, stored heat is discharged before activating CHP, gas boiler, and finally the electric boiler. Electricity demand is met initially through contracted futures supply, then CHP generation if available. If CHP electricity is available but currently not needed, BESS is charged. If needed, the battery is discharged before purchasing electricity from the day-ahead market. Cooling demand is handled by the compression chiller.

If new PV capacity is installed, PV generation is prioritized over CHP electricity. This strategy is modelled based on Section 2.2 and the weights summarized in Table 2. The numerical values are chosen as exponentially separated priority levels (powers of three), so that the hierarchy between commodities and, within each commodity, between assets remains strict even after normalization. Negative values are assigned to storage charging actions to ensure that charging is only selected once higher-priority supply actions have been satisfied and surplus energy or capacity is available.

Table 2. *Priority-based weights for reactive rule-based control*

Parameter **Commodity** / Asset	w^c	w^c_{k}	$w^c_{\mathrm{k,\,ch}}$
Steam	81		
CHP		3	
Gas boiler		9	
Electric Boiler		27	
Water at 90°C	27		
Heat-pump		3	
Hot water tank (charging)			-12
Hot water tank (discharging)		9	

CHP		27	
Gas boiler		81	
Electric boiler		243	
Electricity	9		
Future		3	
PV		9	
CHP		27	
BESS (charging)			-90
BESS (discharging)		81	
Day-ahead spot market		243	
Cold water	9		
Compression chiller		3	

3.3. Design optimization and scenario description

To support decarbonization and energy flexibility, the brewery considers installing new PV capacity at 735 €/kWp and additional BESS and HWT capacity at 360 €/kWh and 70€/kWh, respectively. Using the RRBC-operated baseline system described in Section 3.2, two scenarios are defined:

- **Design optimization (D_0)**: Optimal sizing of PV, BESS and HWT based on Sec. 2.1, neglecting control constraints.
- **Control-informed design optimization (CID_0)**: Design optimization incorporating rule-based operational constraints as described in Sec. 2.3. Following the framework described in 2.3, following additional constraints occur:

$$P^{\text{Out}}_{Gas\ boiler,\ steam}(t) \leq p^{\text{Out, measured}}_{Gas\ boiler,\ steam}(t). \quad (9)$$

$$P^{\text{Out}}_{El.boiler,\ steam}(t) \leq p^{\text{Out, measured}}_{El.boiler,\ steam}(t). \quad (10)$$

$$P^{\text{Out}}_{CHP,\ steam}(t) \leq p^{\text{Out, measured}}_{CHP,\ steam}(t). \quad (11)$$

$$P^{\text{Out}}_{Heat-pump,\ steam}(t) \geq p^{\text{Out, measured}}_{Heat-pump,\ steam}(t). \quad (12)$$

Operational performance of the designs is evaluated with a rule-based control simulation. Subsequently, D_0 and CID_0 solutions are simulated under RRBC, yielding D_S and CID_S scenarios, accordingly. All optimizations are performed using Gurobi 11 [17] on a Windows 11 system with 32 GB RAM.

4. Results

This section presents a comparative evaluation of the investigated scenarios. First, the resulting optimal system designs, specifically the installed photovoltaic, BESS and HWT capacities, are analyzed. Subsequently, Section 4.2 examines the cost structures underlying these design decisions. Finally, Section 4.3 discusses differences in system operation across the scenarios.

4.1. Optimal design

The optimal design outcomes for both design optimization approaches are illustrated in Figure 4. Two main observations emerge.

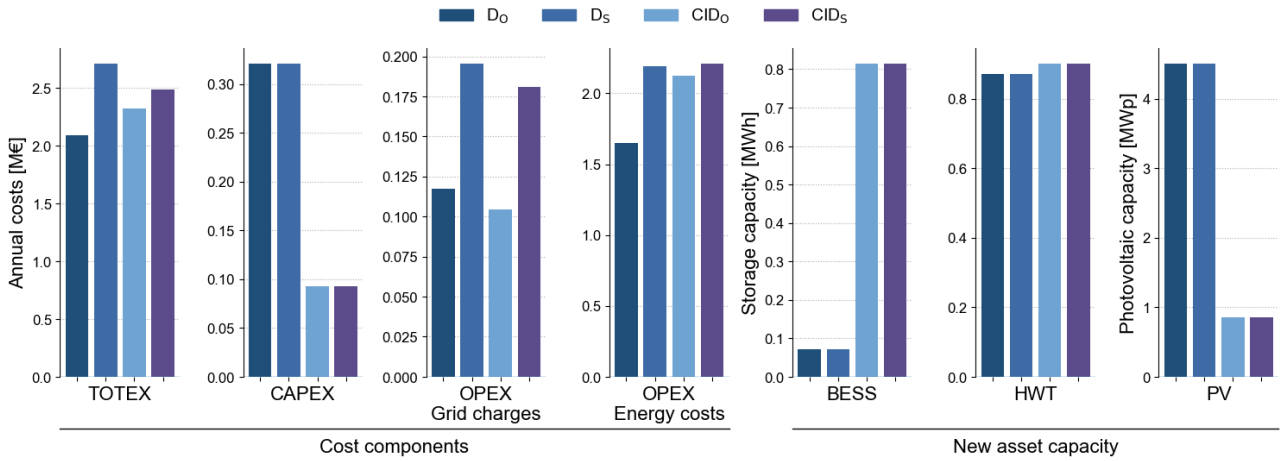

Figure. 4. *Cost difference components and optimal design results for the considered scenarios.*

First, the conventional design optimization D_0, which assumes perfect foresight and fully flexible system operation, invests in much smaller additional BESS and HWT capacities compared to CID_0. Instead, it installs approximately 4.5 MWp of PV capacity. This result reflects the optimizer's ability to exploit the storages' temporal flexibility and align PV generation with demand under idealized operational conditions.

In contrast, the control-informed design optimization CID_0, which explicitly accounts for the constraints imposed by the rule-based control strategy, yields a markedly different investment strategy. Specifically, CID_0 installs a significantly smaller PV capacity of approximately 860 kWp, while simultaneously investing in around 813 kWh and 815 kWh of additional BESS and HWT capacity, respectively. This shift highlights the impact of operational constraints on design decisions, where limited flexibility necessitates alternative investments to maintain system performance.

4.2. Cost components

A detailed examination of the cost components in Figure 4 provides further insight into the observed design differences.

First, consistent with the larger installed PV capacity, the capital expenditure (CAPEX) of the D_0 scenario is more than 3 times higher than that of the CID_0 scenario. This indicates that neglecting operational constraints leads to more aggressive investment strategies, whereas control-informed optimization results in more conservative and targeted capital allocation.

Second, the comparison of total annual system costs (TOTEX) across all scenarios underscores the importance of accounting for real-world control strategies when evaluating investment benefits. While the D_0 scenario predicts annual TOTEX of 2,09 m€, its re-simulation under rule-based control D_S results in a cost increase of 29.6% at 2,71 m€ TOTEX. In contrast, the CID_0 approach estimates more modest TOTEX of 2,32 m€, with its re-simulated counterpart CID_S achieving a slight cost increase of 6.9% at 2,48 k€.

This discrepancy is primarily driven by differences in energy costs and grid charges. When both designs are evaluated under realistic rule-based control, energy costs significantly increase by 32.7% in the D_S scenario compared to the modest increase of 4.0% in the CID_S scenario. Time-coupled cost components, such as monthly grid capacity charges, are notably higher in both re-simulated scenarios D_S and CID_S compared to their respective optimization counterparts. This is attributable to two factors: (i) the assumption of perfect foresight in the design optimization, which enables ideal peak load management, and (ii) the absence of explicit peak-shaving mechanisms in the implemented rule-based control strategy. Consequently, peak demand is not actively minimized in practice, leading to higher grid-related costs. Nonetheless, it is noteworthy to note, that in case of D_0 and D_S, 12.7% of their cost discrepancy is due to the grid charges, whereas in case of CID_0 and CID_S, the same value is at 31.0%. This indicates that the absence of the peak load mechanisms of the RRBC

heavily influences the cost discrepancy in the control-informed case. Overall, the resulting deviations demonstrate that control-informed design optimization provides a more accurate estimation of achievable costs.

4.3. Asset operation

The differences in economic performance can be directly linked to variations in system operation. Figure 5 illustrates the equivalent full cycles of storage systems as well as the extent of PV curtailment.

The differences in storage full cycles are primarily driven by the gap between idealized optimization and practical rule-based operation. In the D_0 and CID_0 scenarios, the optimizer has full foresight and can schedule charging and discharging proactively, which leads to high storage utilization and therefore high equivalent full cycles. Once these designs are simulated under the rule-based controller (D_S and CID_S), storage use drops because the controller reacts only to current surpluses or deficits and follows fixed priority rules instead of anticipating future conditions. This effect is especially strong for the AWT, whose flexibility can be exploited very effectively by optimization but only to a limited extent by the practical controller. Both BESS and HWT show a smaller reduction, since they remain more directly integrated into the electricity-heat supply sequence and are therefore still used regularly even under rule-based control.

The differences in PV curtailment reflect how well each system design matches the actual operating strategy. In the D_0 scenario, curtailment is very low (1.1%) because the optimization assumes perfect foresight and can coordinate PV generation, storage charging, and flexible demand almost ideally. However, when the same design is operated with the practical rule-based controller (D_S), curtailment rises dramatically (88.0%) because the controller cannot anticipate future surpluses and therefore cannot use storage and other assets as effectively to absorb excess PV. The CID_0 scenario performs better under both ideal and practical operation because operational constraints are already considered during the design stage, leading to a more realistic sizing of PV and flexibility assets; therefore, curtailment remains moderate in CID_0 (8.8%) and, although still high, is clearly lower in CID_S (57.6%) than in D_S. Overall, the results show that high PV curtailment is mainly caused by a mismatch between asset sizing and the real operating logic rather than by PV capacity alone.

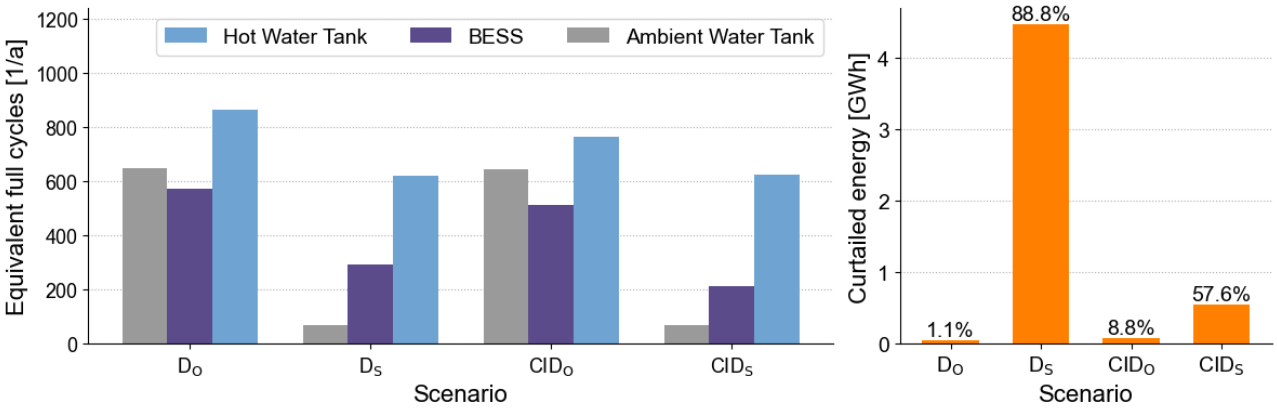

Figure 5. *Storage equivalent full cycles and curtailed PV energy across scenarios.*

Table 3 summarizes the equivalent full-load operating hours of the main thermal assets. The differences in full-load hours reflect the dispatch priorities of the assets in each scenario. Under the practical control logic, the heat pump and CHP are prioritized and therefore operate for more hours per year, while the gas boiler and especially the electric boiler are used less often as backup or last-resort units. This explains why the heat pump and CHP show higher full load hours in the simulated practical scenarios, whereas the gas boiler and electric boiler show lower values. In other words, the change in full-load hours is not only a result of different capacities, but mainly of how often each technology is called upon within the scenario-specific operating strategy.

In contrast, only minor operational changes are observed in the D_S, CID_0, and CID_S scenarios. This is because the introduction of additional PV and BESS capacity may only slightly alter the predefined rule-based dispatch

hierarchy for thermal assets. Consequently, system operation remains largely consistent throughout these scenarios, highlighting the limited flexibility of rule-based control in adapting to new system configurations.

Table 3. Assets' equivalent full-load operating hours [h/a]

Asset	Electric boiler		Gas boiler		CHP		Heat pump	
Scenario								
D_O	**711.2**		**2141.9**		**3688.5**		**4506,3**	
D_S	16.9	↓ **97.6%**	1684.9	↓ **21.3%**	6729.1	↑ **82.4%**	6390.7	↑ **41.8%**
CID_O	13.9	↓ **98.0%**	1697.6	↓ **20.7%**	6706.7	↑ **81.8%**	6188.3	↑ **37.3%**
CID_S	16.9	↓ **97.6%**	1685.1	↓ **21.3%**	6744.4	↑ **82.9%**	6361.1	↑ **41.2%**

↑↓ **x.x%:** relative change compared to Design Optimization scenario D_O

5. Conclusion

This study presents a control-informed design optimization (CID_O) framework for industrial energy systems and evaluated its performance against conventional design optimization (D_O) using a real-world brewery case study. By explicitly incorporating rule-based operational constraints into the design phase, the proposed approach reduces the fundamental mismatch between idealized optimization assumptions and practical system operation.

The results demonstrate that operational strategy has a decisive impact on optimal system design. While D_O favors a PV-dominated solution with approximately 4.5 MWp and only limited additional BESS storage, CID_O leads to a more conservative but operationally robust design with around 860 kWp of PV, 813 kWh of additional BESS and 815 kWh of additional HWT capacity. This shift reflects the limited flexibility of the rule-based EMS, which cannot exploit temporal mismatches between generation and demand as effectively as full-foresight optimization.

A key finding is the substantial discrepancy between expected and realized system performance when operational constraints are neglected. CID_O approach provides more conservative but robust investment decisions, resulting in cost estimates that are more closely aligned with actual system performance. This highlights the importance of integrating operational behavior into design optimization to avoid misleading investment signals. Quantitatively, the mismatch is substantial: when the conventionally optimized design is re-evaluated under rule-based control, realized TOTEX increases by 29.6%, and PV curtailment rises from 1.1% to 88.0%.

Furthermore, the analysis reveals that renewable energy integration, particularly high shares of PV, strongly depends on the availability of advanced control strategies. Under rule-based control, large portions of PV generation are curtailed due to limited system flexibility and suboptimal dispatch logic. In contrast, optimization-based or predictive control strategies can further enhance renewable utilization by enabling anticipatory scheduling of flexible assets such as storage systems and controllable loads. Consequently, the effectiveness of renewable integration is not solely a function of installed capacity but is critically determined by the underlying energy management system.

The findings also emphasize the role of storage technologies as enablers of flexibility under constrained operation. While idealized optimization can exploit existing and new system flexibility in an optimal way and with limited storage-investments, real-world control limitations necessitate increased storage capacity to compensate for limited controllability and foresight. This underscores the interdependence between system design, control strategy, and flexibility provision.

6. Outlook

Future work should extend the proposed framework by incorporating advanced control strategies, such as model predictive or learning-based energy management systems, to better capture the value of operational flexibility. Additionally, integrating uncertainty in demand, renewable generation, and market conditions would improve the robustness of design decisions. Expanding the system scope to include further sector coupling options and investigating the practical implementation of more sophisticated control approaches in industrial settings will be essential to support reliable and cost-effective decarbonization pathways.

References

[1] International Energy Agency. Tracking SDG7: The Energy Progress Report, 2025. Paris, France: IEA; 2025. Available at: <https://www.iea.org/reports/tracking-sdg7-the-energy-progress-report-2025> [accessed 27.3.2026].

[2] European Environment Agency, Flexibility solutions to support a decarbonised and secure EU electricity system. EEA/ACER Report 09/2023. Copenhagen, Denmark: European Environment Agency; 2023. Available at: <https://www.eea.europa.eu/en/analysis/publications/flexibility-solutions-to-support> [accessed 27.3.2026].

[3] Mancò G., Tesio U., Guelpa E., Verda V. A review on multi energy systems modelling and optimization. Applied Thermal Engineering 2024;236:121871. doi:10.1016/j.applthermaleng.2023.121871.

[4] Fallmann M., Stanger L., Fischer M., Kureck M., Schirrer A., Hofmann R., et al. Experimental validation of mixed-integer model predictive control for energy management in an industrial food processing plant. Case Studies in Thermal Engineering 2025;75:106988. doi:10.1016/j.csite.2025.106988.

[5] Urban K.L., Scheller F., Bruckner T. Suitability assessment of models in the industrial energy system design. Renewable and Sustainable Energy Reviews 2021;137:110400. doi:10.1016/j.rser.2020.110400.

[6] Atabay D. An open-source model for optimal design and operation of industrial energy systems. Energy 2017;121:803-21. doi:10.1016/j.energy.2017.01.030.

[7] Karlsson M. The MIND method: a decision support for optimization of industrial energy systems - principles and case studies. Applied Energy 2011;88(3):577-89. doi:10.1016/j.apenergy.2010.08.021.

[8] Paudyal S., Cañizares C.A., Bhattacharya K. Optimal operation of industrial energy hubs in smart grids. IEEE Transactions on Smart Grid 2015;6(2):684-94. doi:10.1109/TSG.2014.2373271.

[9] Cuisinier E., Lemaire P., Ruby A., Bourasseau C., Penz B. Impact of operational modelling choices on techno-economic modelling of local energy systems. Energy 2023;276:127599. doi:10.1016/j.energy.2023.127599.

[10] Brisson J., Vallée M., Piguet A., Lemaire P., Phouratsamay S.-L. Impact of levels of modeling details in energy system sizing optimization: a case study. Energy 2025;332:136033. doi:10.1016/j.energy.2025.136033.

[11] Kachirayil F., Weinand J.M., Scheller F., McKenna R. Reviewing local and integrated energy system models: insights into flexibility and robustness challenges. Applied Energy 2022;324:119666. doi:10.1016/j.apenergy.2022.119666.

[12] Restrepo M., Cañizares C.A., Simpson-Porco J.W., Su P., Taruc J. Optimization- and rule-based energy management systems at the Canadian Renewable Energy Laboratory microgrid facility. Applied Energy 2021;290:116760. doi:10.1016/j.apenergy.2021.116760.

[13] Höttecke L. Sustainable design of industrial energy supply systems - development of a model-based decision support framework [dissertation]. Darmstadt, Germany: Technische Universität Darmstadt; 2023. Available at: <https://tuprints.ulb.tu-darmstadt.de/entities/publication/9927bb31-3048-4782-9c0e-24f73fd7987e> [accessed 27.3.2026].

[14] Lipka J.B., Höttecke L., Stursberg P., Metzger M., Heger H.-J., Niessen S. Including batch scheduling flexibility in industrial energy system design and dispatch optimization: a case study of a brewery. Energy 2026;346:140295. doi:10.1016/j.energy.2026.140295.

[15] Lipka J.B., Höttecke L., Stursberg P., Metzger M., Heger H.-J., Niessen S. Energy flexibility from industrial supply systems based on different optimization horizons - an application to a German manufacturing industry. In: ECOS 2024: Proceedings of the 37th International Conference on Efficiency, Cost, Optimization, Simulation, and Environmental Impact of Energy Systems; 2024 Jun 30-Jul 5; Rhodes, Greece. 2024. p. 1854-65. doi:10.52202/077185-0159.

[16] Lipka J.B., Höttecke L., Stursberg P., Metzger M., Heger H.-J., Niessen S. Optimal energy system design for brewing site decarbonization via electrification. In: ECOS 2025: Proceedings of the 38th International Conference on Efficiency, Cost, Optimization, Simulation, and Environmental Impact of Energy Systems; 2025 Jun 29-Jul 4; Paris, France. 2025.

[17] Gurobi Optimization, LLC. Gurobi Optimizer Reference Manual. 2025. Available at: <https://docs.gurobi.com/projects/optimizer/en/current/index.html> [accessed 27.3.2026].

Appendix A

Table A.1. Asset model parameters for the considered case study

Parameter	$p_{\mathrm{R},k}$	$c_{\mathrm{R},k}$	η_k	$\eta_k^{\mathrm{in},2}$	$\eta_k^{\mathrm{out},2}$	η_k^{ch}	η_k^{dch}	η_k^{self}	$pl_k^{\min}$	w_k^{Energy}	w_k^{Peak}
Unit	[MW]	[MWh]	[-]	[-]	[-]	[-]	[-]	[-]	[-]	[ct/kWh]	[€/kW/month]
Futures	0.3									7.96	

Spot market								SM_{25}^{*}		
CHP feed-in								$-0.9*SM_{25}$		
PCC			1					2.24	12	
Gas grid								8.5		
CHP	1.2		0.446	0.422			0.4			
Gas boiler	3		0.95							
Electric boiler	4		0.98							
Heat-pump	0.8		3.68	1			0.2			
Heat exchanger	10		1							
BESS	0.62	0.62			0.95	0.85				
Ambient water tank	2	2			1	1	0.01			
Hot water tank	3	3			1	1	0.01			

* - SM_{25}: Day-ahead spot market price in Germany, 2025